Development of a new LED-based solar simulator for building-integrated photovoltaic characterization

Elisa Belloni*
Dipartimento di Ingegneria
University of Perugia
Perugia, Italy
elisa.belloni@unipg.it

Marco Casini
Dipartimento di Ingegneria dell'Informazione e Scienze Matematiche, University of Siena
Siena, Italy
casini@ing.unisi.it

Antonio Faba
Dipartimento di Ingegneria
University of Perugia
Perugia, Italy
antonio.faba@unipg.it

Antonino Laudani
Dipartimento di Ingegneria Elettrica, Elettronica e Informatica
University of Catania
Catania, Italy
alaudani@unict.it

Gabriele Maria Lozito
Dipartimento di Ingegneria dell'Informazione
University of Firenze
Firenze, Italy
gabrielemaria.lozito@unifi.it

Abstract— **Building-Integrated Photovoltaics (BIPV) is an effective method of producing renewable energy providing also one or more functions of the building envelope. Among PV solutions, bifacial PV module technology captures sunlight from both the front and rear sides, increasing the module's power output per square meter. The evaluation of the overall performance of these cells is not easy because the irradiance conditions on the back side is variable. This article describes the design of a versatile light-emitting diode (LED) based solar simulator with independently controlled high-power LEDs. This laboratory-scale setup is designed to be suitable for the tests of bifacial cells reproducing the lighting conditions typical of the back side of the cells. To this aim an office configuration with bifacial PV glazing windows was simulated in DIALux to analyze the irradiance and lighting conditions on the glazing pane from inside environment. The results are used to choose the geometry features, the materials, and the operation mode of the lamps of the simulator.**

Keywords— Bifacial photovoltaic cells, Building Integrated Photovoltaics (BIPVs), Electrical model, Illuminances, Light-emitting diodes (LEDs), Solar simulator

I. INTRODUCTION

As the use of solar energy increases, performance testing is one of the most important aspects to ensure the safety of photovoltaic tools. Therefore, considering future energy standards, it is important to use solar simulators that allow the reproduction of real sunlight spectral values. The main components of solar simulators used in photovoltaic panel testing are light sources. Two types of solar simulator are widely used today: steady-state and flash. In particular, a steady-state simulator provides accurate measurements for solar devices with long time constants, but it can cause thermal control problems and has high operating and maintenance costs. Flash simulators have lower running costs but higher initial investment costs due to the specific type of lamps to be used; another advantage is the lower impact on device temperature [1]. The choice of the lamps is a critical aspect and many research works proposed alternative designs of the solar simulator and different types of lighting sources such as carbon arc, sodium vapor, argon arc lamps, quartz-tungsten halogen lamps, mercury xenon lamps, xenon arc, xenon flash lamps, LED, and laser light sources [2-4]. To evaluate the performance of photovoltaic devices, they are rated under Standard Test Conditions (STC). These conditions correspond to an irradiance of 1000 W/m^2 and a device temperature of 25°C [5].

Building-integrated photovoltaic (BIPV) systems are a suitable solution for the diffusion of renewable energy and distributed generation [6-8]. They are generally applied on roofs (modules on a lightweight substrate, modules with integrated solar cells as roofing elements, photovoltaic roof tiles), but they can also be applied on facades (BIPV cladding walls and curtain walls, glazing transparent facades) and accessories (BIPV shading devices and balconies). In buildings with large glazing areas, the application on the transparent envelope is also interesting, considering that they can act as shading to limit the glare effect and summer cooling consumption [9,10]. Among the recent technologies, bifacial PV cells are effectiveness for this application and not very expensive with respect to other innovative treatments for glazing [11]. Nevertheless, the increasing of productivity obtained from the back side is not easy to be determined because of the particular conditions that may arise.

For these reasons, it could be interesting to develop a device able to reproduced the irradiance conditions on the back side of PV-bifacial cells that are not the same we have with the global solar radiation on horizontal surface. This is particularly interesting when characterizing the overall performance of PV modules with bifacial cells. Bifacial cells can also be used as glazing panes, in which case the irradiance distribution on the back side results from the illuminance distribution in the building's internal environment.

In this context, the present paper presents a preliminary design and development of an experimental solar simulator for analyzing irradiance conditions in an indoor environment. The simulator was driven by lighting simulations developed in the DIALux program. An office room was considered as a case study: the irradiance and illuminance distributions on the glazing surface from the rear were studied and used for the calibration of the solar simulator, the choice of lamps and their dimming. The paper is organized as follows: section II

This project received funding from the European Union Next - generation EU: project PRIN (Progetti di Ricerca di Rilevante Interesse Nazionale) 2022 PNRR; Title project: MOST4BIPV - Modeling and Optimization of Smart Technologies for Building Integrated Photovoltaics, code: P20224JSA7.

979-8-3503-5518-5/24/$31.00 ©2024 IEEE

describes the methods adopted for the analysis, both for the lighting/irradiance and for the electric points of view. Section III shows all the results obtained for the analysis, the preliminary project for the solar simulator and, specifically, the electricity behavior of the bifacial cells. Conclusions and future development are finally summarized in section IV.

II. Materials and Methods

A. The case study and the implemented BIPV technology

The room chosen as case study is an office located in Italy center with two balcony glazing doors in the south-west façade. The total area of the office is 19.5 m^2 and the height is about 2.9 m. The total transparent area is 2.75 m^2 and about 0.85 m^2 are considered covered by PV-bifacial cells that are also useful as shading system for the occupants. Two glazing PV panels with dimensions 65 x 65 cm^2 are positioned in the upper level of the window. A total number of 16 bifacial monocrystalline cells (peak power of 3.75 Wp, total efficiency equal to 21%) are connected in series, spaced 2.5 cm each other. The total peak power of the PV glazing system is 60 Wp. Fig.1(a) shows the photo of the office in real conditions and specifically the west façade. Fig.1(b) presents the configuration of the windows with PV bifacial cells integrated. The artificial lighting system comprises four square LED lamps measuring 59 x 59 cm, each with a total power of 45 W and an efficiency of 95 lm/W. The lamps can be controlled in pairs to illuminate the separate workspaces on the right and left sides of the office.

B. DIALux simulations

The case study was implemented in a lighting simulation program (DIALux 4.13 [12]) to get a complete view of the illuminance values on the surfaces and, in particular, on the glazing area with bifacial PV cells from the back side. The contribution in terms of illuminance and solar radiation is due to the artificial LED lamps installed in the room and on the sunlight reflected from the surfaces. This second contribution depends on the month of the year and the hour of the days. Therefore, many simulation scenarios were examined in order to analyze the irradiance on the PV cells.

Three artificial lighting scenes were reproduced considering two control groups of the lamps in the office (evening/night period when the sunlight is not present): 4 lamps on (A4), 2 lamps on (right side) (A2r), 2 lamps on (left side) (A2l) as visible in Fig.2(a). Moreover, the contribution of sunlight is examined in reference days for every season: March 21, June 21, September 21, and December 21 (light scenes named SM21, SJ21, SS21, and SD21, respectively). Finally, mixed scenarios are analyzed considering both the kinds of light: in some days in the time period 3 p.m. – 5 p.m. and when it is cloudy the switching-on of the artificial lamps is necessary.

The best and the worst scenarios in terms of illuminance values are selected and considered in order to reproduce these conditions with the experimental solar simulator. In particular, the case with only artificial lamps (A4) and the case with higher irradiance on the PV system due to sunlight and lamps (A4-SJ21) are considered in this work for the sake of brevity. The maps of illuminance (lm/m^2=lx) obtained from this analysis were transposed in terms of irradiance (W/m^2) by means of conversion factors [13,14]. Fig.2(b) shows the rendering 3D view of the simulated room.

Fig. 1. a) Photos of the office windows considered as case study: outside view - on the left; view from the indoor environment - on the right; b) front side view of the façade and positioning of the PV-glazing system in the window.

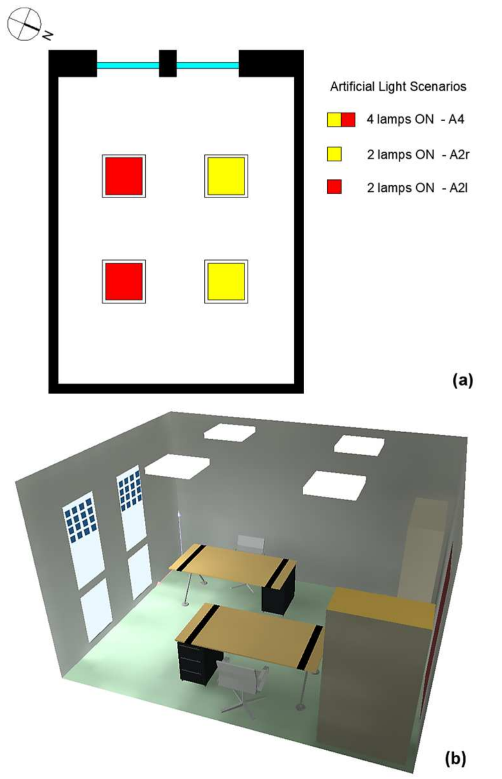

Fig. 2.(a) Artificial lighting scenes simulated in DIALux; (b) 3D rendering view of the office.

C. Preliminary design of the solar simulator

DIALux Evo 12.0 [12] software is generally used for architectural lighting and for the design of indoor, outdoor, and street lighting systems. In this platform a solar simulator case was designed and modelled. This program was chosen because it allows the detailed modelling of lamps in terms of power, emitted flux, light spectrum, and photometric solids.

An open aluminum cube box 80x80x80 cm was modelled and a plate with 16 LEDs mounted on an aluminum cover is designed to close the box. Different commercial LEDs were selected from the manufacturer websites and they were simulated: lamps with a spectral distribution similar to the sun behavior were chosen with a maximum absorbed peak power equal to 6W. Each one can be also dimmable in order to regulate the emitted power and flux. A calculation surface is positioned in the bottom side of the simulator and represents the PV system to be tested. The laboratory solar simulator has been designed to reproduce irradiance conditions similar to the backsides of bifacial PV glazing systems and has been therefore calibrated on the basis of the previous results (section II.B) (Fig.3): the model and the regulation of the lamps can be fixed on the basis of the irradiance and illuminances obtained on the test surface that should be the same as we have on the backside of the office window. A schematic layout of the solar simulator is shown in Fig.3(a); Fig.3(b) shows the features of the LED lamps chosen as sources.

D. Electric modelling method

To understand the electrical implications of the non-uniform irradiance distribution an electrical model of individual cells and their interconnection was implemented. The model is based on the equivalent circuit model for a silicon PV device, the Single-Diode model. The model is shown in Fig.4(a) and its electrical current-voltage characteristic is given by:

$$i_{pv} = I_{irr} - I_o\left(e^{\frac{v_{pv}+R_S*i_{pv}}{n*V_T}} - 1\right) - \frac{v_{pv}+R_S*i_{pv}}{R_{sh}} \qquad (1)$$

where the five parameters $\{R_s, R_{sh}, I_{irr}, I_o, n\}$ are respectively the series and shunt resistance, the photogenerated current, the inverse saturation current and the ideality factor of the diode. The model current-voltage relation is implicit since the current depends on the diode voltage $v_d = v_{pv} - Rs * i_{pv}$. The model can also be seen as a unique non-linear voltage-controlled-current-source (v_{CCS}) dependent on v_d, as shown in Fig.4(b). The model parameters are in general identified at standard reference conditions (irradiance of $G = 1kW/m^2$ and $T = 298.15K$) and then updated using a set of well-accepted equations from literature [15-16]. To create a model implementation compatible with further simulation and optimization tasks, the model was implemented in a circuit simulation environment. In particular, the PLECS simulator was used. The choice for the environment is due to different reasons. First, the model is not implemented directly in the PLECS libraries, nor it can be implemented easily due to the piecewise-linear approach used to implement diodes in the simulator. Second, PLECS is a very diffused simulation system for power converters, which makes this model useful for power PV applications. It should be noted that even if the current study is focused on a low-power application, the implementation of the single-diode model scales without issues to PV sources of any size. Third, PLECS implements a thermal model that can run in co-simulation with the electrical model, opening the possibility of expanding the current PV model also including the temperature characteristics of the panel, even at cell level.

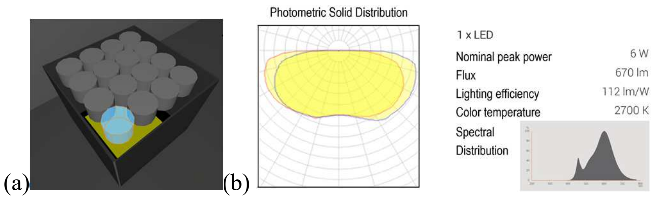

Fig. 3. (a) Schematic view of the solar simulator modelled in DIALux Evo; (b) main characteristics of the selected LED lamp.

The model implementation uses the VCCS representation of Fig.4(b), directly exploiting the possibility of including a C code in the electrical solver. The individual cell electrical model is given by the sub-circuit shown in Fig. 5. The C-Script block computes the updated parameters for variable irradiance and temperature conditions given the reference ones, and from those, the VCCS current i_g. The extract of the code for the computation is given below:

LISTING 1 - C-SCRIPT OUTPUT FUNCTION CODE

```
#include <stdio.h>
#include <math.h>
#define RsRef InputSignal(0, 0)
#define RshRef InputSignal(0, 1)
#define IirrRef InputSignal(0, 2)
#define IoRef InputSignal(0, 3)
#define nRef InputSignal(0, 4)
#define alpha InputSignal(0, 5)
#define G InputSignal(0, 6)
#define T InputSignal(0, 7)
#define vdiode InputSignal(0, 8)
#define Current OutputSignal(0,0)
#define Rsh OutputSignal(0,1)
#define Rs OutputSignal(0,2)

const float k = 1.380648521e-23;
const float q = 1.60217662e-19;
const float Vt = k*T/q;
const float kEv = 8.61673324e-5;
const float Eg = 1.166 - 4.73e-4 * T * T/(T+636);
const float Eg_ref = 1.166 - 4.73e-4 * 298.15 *
298.15/(298.15+636);

float Iirr = IirrRef*(G/1000)*(1+alpha*(T-
298.15));
float Io =
IoRef*(T/298.15)*(T/298.15)*(T/298.15)*exp(Eg_ref/
(kEv*298.15) - Eg/(kEv*T));
float n = nRef;

Rs = (RsRef);
Rsh = (1000/(G+0.001))*(RshRef);
Current = Iirr - Io*(exp(vdiode/(n*Vt))-1);
```

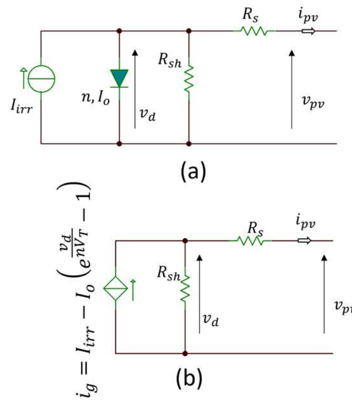

Fig. 4. Original single-diode equivalent circuit model (a) and a modified version featuring a single non-linear VCCS for both photocurrent and diode current (b).

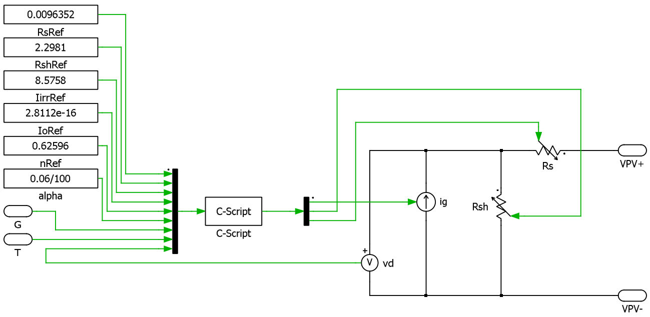

Fig. 5. Individual cell electrical model featuring the cell reference parameters, the input ports for the environmental conditions of irradiance and temperature, the C-Script for the parameters update and current computation, and the electrical ports.

III. Results and Discussion

A. Lighting and irradiance results

The illuminance maps obtained on the back side of the PV glazing system are shown in Fig. 6. Specifically, the scenarios with only artificial lighting on are reported (A4, A21, and A2r) together with the case with maximum irradiance obtained with both artificial and solar contributions in summer (A4-SJ21). In general, a uniformity coefficient of about 87% is observed with higher values on the lower part of the surface: maximum values of about 1200 lx are obtained in the more brightened conditions. Fig.7 represents two natural lighting scenarios without the lamps contribution in March and December: when only sunlight is present a higher homogeneity of illuminance distribution is obtained (100%) thank to the only effect of the diffuse light inside the office. Considering these distributions, the corresponding irradiances (W/m^2) on the surfaces are quite different based on the type of lighting sources, seasons and time of the day [13,14]. When only the sunlight is present, maximum radiation on the vertical surface equal to 1.5 W/m^2 and 3.5 W/m^2 are obtained in Winter and Spring, respectively; among the simulations carried out, the maximum values reachable in these conditions are about 8-9 W/m^2. The artificial lighting contribution allows an increasing of the total irradiance up to about 29-30 W/m^2: these scenarios were reproduced in the solar simulator in the next paragraph.

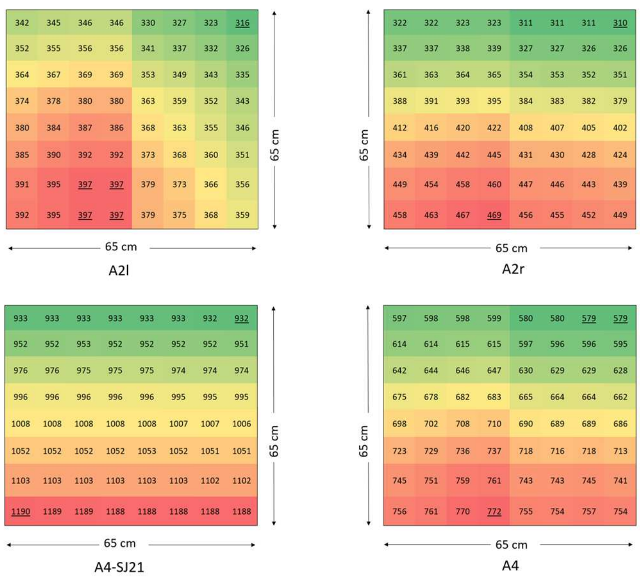

Fig. 6. Illuminance distribution in [lx] on the bifacial PV- glazing system surface in artificial and mixed lighting scenarios.

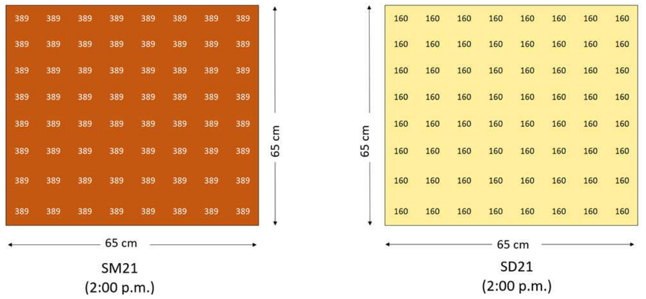

Fig. 7. Illuminance distribution in [lx] on the bifacial PV- glazing system surface in two natural lighting scenarios: March 21 on the left, December 21 on the right.

B. Solar simulator scenarios

To recreate the irradiance distribution of the tested surface using the solar simulator, numerous simulations were conducted in DIALux EVO. The power emitted from the lamps and the corresponding lighting fluxes were adjusted until the desired irradiance values and distribution were achieved on the calculation surface. To ensure brevity, this analysis focuses solely on the brightest case. Fig.8 shows the final lighting irradiance on the cells in two scenarios. To achieve the specific configuration in Fig.8(a), the 4 LED lamps on the bottom line should be regulated to 5 W (560 lm in terms of flux), while the other 12 lamps should emit 450 lm (equivalent to 4 W). The electric behavior of the cells in this case will be presented in Section III.B.

C. Electric behavior of the PV glazing system

The cell parameters were extracted starting from the datasheet values of open circuit voltage v_{OC}, short circuit current i_{SC} and maximum power voltage v_{mp} and current i_{mp} (Tab. I). A sensible value for the temperature dependence of the short circuit current α was assumed. Extraction was performed using circuit identification techniques implemented in the online parameters extractor available at [17].

The individual cell model is then included in a larger circuit featuring 16 cells connected in series (Fig.9), each subject to a different individual irradiance and a uniform temperature that, for simplicity, is assumed as 298.15K, i.e. standard reference temperature. The panel characteristic is extracted using a simple voltage source to investigate both current and delivered power for all voltages between short and open circuit.

Two different scenarios are investigated for the irradiance on bifacial PV panels. In the first case, the irradiance is obtained from both the artificial LEDs in the rooms and the sun radiation during Spring (June 2023) (case A, blue line in Fig.10). In the second scenario, the irradiance distribution is provided only by the LED lamps in the indoor environment (during the evening and night) (case B, red line in Fig.10). From the resulting curves in Fig.10 it is evident that the back side of the PV panel can maintain a 0.5 W production even in the absence of outdoor lighting, i.e. during the night.

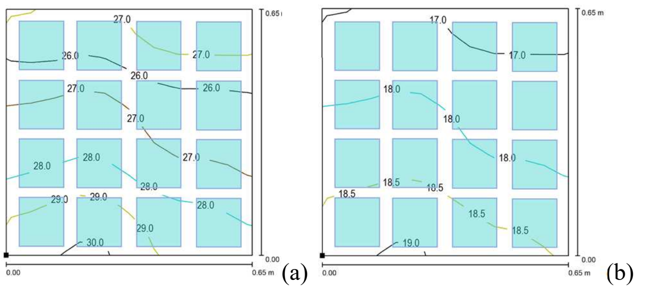

Fig. 8. Irradiance distribution in [W/m^2] reproduced on the tested surface with the solar simulator in the brightest conditions: (a) scenario 4A-SJ21; (b) scenario 4A.

TABLE I. DATASHEET AND SINGLE DIODE PARAMETERS FOR THE PV CELL

Datasheet Parameters		***Single Diode Model***	
$v_{OC}[V]$	0.60	$R_{s,ref}[\Omega]$	0. 0096352
$i_{SC}[A]$	8.53	$R_{sh,ref}[\Omega]$	2.2981
$v_{MP}[V]$	0.48	$I_{irr,ref}[A]$	8.5758
$i_{MP}[A]$	7.79	$I_{o,ref}[A]$	2.8112×10-16
$\alpha[\%/K]$	0.06	n_{ref}	0.62596

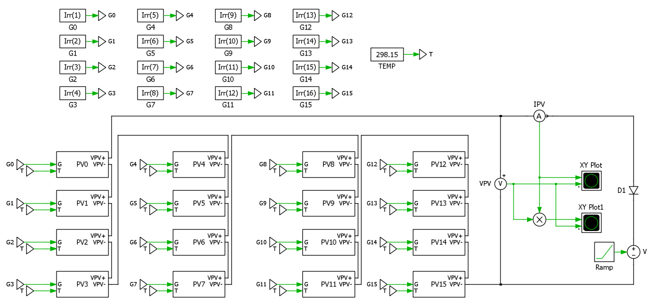

Fig. 9. Full PLECS implementation of the PV panel featuring the 4x4 disposition of 16 cells with non-uniform irradiance.

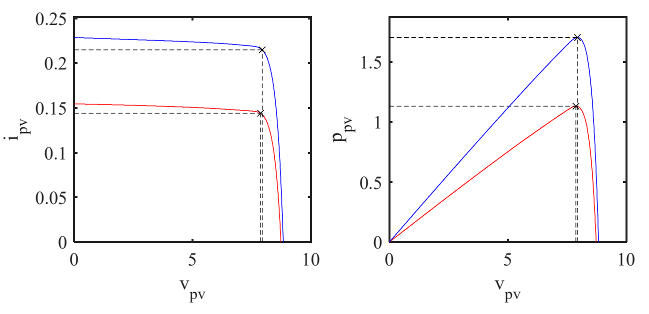

Fig. 10. Current-Voltage (left) and Power-Voltage (right) characteristics for the first scenario (blue curve) and second scenario (red curve). Maximum power is always delivered at $v_{mp} \approx 8V$ and is 1.70W in the first case and 1.13W in the second case.

IV. CONCLUSIONS

This paper proposes a laboratory solar simulator capable of simulating the lighting conditions on PV glazing systems. The proposed novel approach considers the forecasting analysis of irradiance reachable on the backside of bifacial PV glazing systems by means of illuminance/irradiance simulations. The design process and the preliminary configuration have been defined on the basis of DIALux simulation results obtained from modelling a typical office. DIALux has great potential for reproducing both natural and artificial lighting scenes and it could be a useful instrument for this purpose. The illuminance distributions are variable depending on the time of the year (sunlight contribution) and the LED lamps installed in the office itself. The power delivered by the back of a bifacial PV device at night is very low compared to the surface area. When regulated by a step-down converter with 95% efficiency, at 3.3V, the expected available current is around 325mA. Such current is, however, largely sufficient to supply the energy demand of a modern smart sensor implemented on a microcontroller such as the STM32 [18]. Such microcontroller features network capabilities at very low current absorption. For example, the core and processors can be kept alive in modem-sleep mode absorbing less than 20mA, and active transmission/reception of packets can be performed at 200mA.

The limitations of the proposed methodology can be overcome by means of experimental measurements to be carried out in the office under a variety of lighting conditions, including both artificial and natural lighting scenarios. Moreover, this scenario can vary depending on the orientation of the rooms and when glazing surfaces are positioned in opposite sides with the transparent envelope partially replaced with bifacial PV-glazing systems. The proposed irradiance simulator can be tuned in order to reproduce these particular lighting and radiation conditions.

REFERENCES

[1] M. Bliss, T.R. Betts, R. Gottschalg, "An LED-based photovoltaic measurement system with variable spectrum and flash speed," Solar Energy Materials and Solar Cells, vol. 93, Issues 6–7, 2009, pp. 825-830.

[2] M. Tavakoli, F. Jahantigh, H. Zarookian, "Adjustable high-power-LED solar simulator with extended spectrum in UV region," Solar Energy, vol. 220, 2021, pp.1130-1136.

[3] Ž. Vosylius, D. Antonovič, A. Novičkovas, E. Gaubas, V. Tamošiūnas, "Rational selection of light sources for LED-based solar simulators," Solar Energy, vol. 265, 2023, 112064.

[4] V. Esen, Ş. Sağlam, B. Oral, "Light sources of solar simulators for photovoltaic devices: A review," Renewable and Sustainable Energy Reviews, vol. 77, 2017, pp.1240-1250.

[5] R. Peamsuwan, P. Waramit, I. Worapun, B. Krittacom, T. Phoo-Ngernkham, R. Luampon, "Investigation of tungsten halogen lamp for possible usage as heat source for testing solar collector," Energy and Built Environment, vol. 5, Issue 4, 2024, pp.517-528.

[6] P. Marrone, F. Fiume, A. Laudani, I. Montella, M. Palermo, M., & F.R. Fulginei, "Distributed Energy Systems: Constraints and Opportunities in Urban Environments," Energies 2023, 16, 2718.

[7] F. Corti et al. "Dynamic Analysis of a Supercapacitor DC-Link in Photovoltaic Conversion Applications," Energies 2023, 16, 5864.

[8] V. Lucaferri, M. Quercio, A. Laudani, F.R. Fulginei, "A Review on Battery Model-Based and Data-Driven Methods for Battery Management Systems," Energies 2023, 16, 7807.

[9] E. Moretti, E. Belloni, F. Merli, M. Zinzi, C. Buratti, "Laboratory and pilot scale characterization of granular aerogel glazing systems," Energy and Buildings, 202, 2019, 109349.

[10] E. Belloni, C. Buratti, F. Merli, T. Ihara, "Thermal-energy and lighting performance of aerogel glazings with hollow silica: Field experimental study and dynamic simulations," Energy and Buildings, 2021, 243, 110999.

[11] C. Buratti, E. Moretti, E. Belloni, "Nanogel Windows for Energy Building Efficiency." In: Pacheco Torgal, F., Buratti, C., Kalaiselvam, S., Granqvist, CG., Ivanov, V. (eds) Nano and Biotech Based Materials for Energy Building Efficiency. 2016. Springer, Cham.

[12] DIALux evo program. Retrieved March 10 2024 from https://www.dialux.com/en-GB/dialux.

[13] P. R. Michael, D. E. Johnston, and W. Moreno, “A conversion guide: solar irradiance and lux illuminance,” Journal of Measurements in Engineering, 2020, Vol. 8, No. 4, pp. 153–166.

[14] Conversion Lux To W/m2. Available online at: https://www.domat-int.com/en/conversion-lux-to-w-m2.

[15] A. Laudani et al. “On the Identification of One diode PV model by reduced forms and different metrics”. In: 2023 3rd International Conference on Electrical, Computer, Communications and Mechatronics Engineering (ICECCME). IEEE. 2023, pp. 1– 7.

[16] W. De Soto, S.A. Klein, W.A. Beckman, “Improvement and validation of a model for photovoltaic array performance,” Solar energy, 2006, 80(1), 78-88.

[17] PV-model. Available online at: https://pvmodel.umh.es/

[18] F. Corti, A. Laudani, G.M. Lozito, A. Reatti, A. Bartolini, L. Ciani, “Model-based power management for smart farming wireless sensor networks.” IEEE Transactions on Circuits and Systems, 2022, 69(5), 2235-2245.